

1 **Water equivalent thickness values of materials used in beams of protons,**
2 **helium, carbon and iron ions**

3 **Rui Zhang^{1,2}, Phillip J Taddei², Markus M Fitzek^{3,4} and Wayne D Newhauser^{1,2}**

4

5 ¹ Graduate School of Biomedical Sciences, The University of Texas at Houston, 6767
6 Bertner, Houston, TX 77030, USA

7 ² Department of Radiation Physics, Unit 1202, The University of Texas M. D. Anderson
8 Cancer Center, 1515 Holcombe Boulevard, Houston, TX 77030, USA

9 ³ Midwest Proton Radiotherapy Institute, 2425 Milo B Sampson Lane, Bloomington, IN
10 47408, USA

11 ⁴ Indiana University School of Medicine, 535 Barnhill Drive, RT 041, Indianapolis, IN
12 46202, USA

13

14 Corresponding author: Wayne D. Newhauser, Ph.D., Department of Radiation Physics,
15 The University of Texas M. D. Anderson Cancer Center, 1515 Holcombe Blvd, Unit
16 1202, Houston, TX 77030. Tel: 713-563-1520; Fax: 713-563-6949; E-mail:

17 wnewhaus@mdanderson.org

18

19 Short Title: Water equivalent thickness of heavy charged particle beams

20

21

22

23

24 **Abstract**

25 Heavy charged particle beam radiotherapy for cancer is of increasing interest because it
26 delivers a highly conformal radiation dose to the target volume. Accurate knowledge of
27 the range of a heavy charged particle beam after it penetrates a patient's body or other
28 materials in the beam line is very important and is usually stated in terms of the water
29 equivalent thickness (WET). However, methods of calculating WET for heavy charged
30 particle beams are lacking. Our objective was to test several simple analytical formulas
31 previously developed for proton beams for their ability to calculate WET values for
32 materials exposed to beams of protons, helium, carbon and iron ions. Experimentally
33 measured heavy charged particle beam ranges and WET values from an iterative
34 numerical method were compared with the WET values calculated by the analytical
35 formulas. In most cases, the deviations were within 1 mm. We conclude that the
36 analytical formulas originally developed for proton beams can also be used to calculate
37 WET values for helium, carbon, and iron ion beams with good accuracy.

38

39 **Keywords:** water equivalent thickness, heavy charged particle, radiation therapy

40 **PACS numbers:** 14.20.Dh, 34.50.Bw, 61.85.+p, 14.20.Dh, 82.39. Jn

41 **Conflict of Interest:** none

42

43

44

45

46

47 **1. Introduction**

48 Interest in heavy charged particle beam therapy has gradually increased since
49 Wilson (1946) first proposed using particle beams in radiation therapy; Wilson pointed
50 out that the properties of specific ionization of heavy charged particles could be used for
51 medical and biological applications. Since then, heavy charged particle beams used in
52 radiotherapy have included protons and heavier ions such as carbon ions (Goitein *et al*
53 2002, Jakel *et al* 2003, Amaldi and Kraft 2005, Schulz-Ertner *et al* 2006, Schulz-Ertner
54 and Tsujii 2007). The most important advantage of heavy charged particles is that they
55 deposit most of their energy within a narrow range represented by the Bragg peak; this
56 predictable deposition of dose can be utilized to spare normal tissues and kill malignant
57 cells. In addition, the energies of heavy charged particle beams can be adjusted using
58 modulating materials to treat any part of tumors within a patient.

59 During quality assurance testing with phantoms and radiotherapy treatment
60 planning, liquid or solid water is frequently used to represent patient tissue (either by
61 itself or in combination with other materials) for beam range and absorbed dose
62 measurements, and water equivalent thickness (WET) or water equivalent ratio (WER) is
63 often used to characterize the beam penetration range. For highly conformal heavy
64 charged particle beam therapy with millimeter accuracy, it is very important to determine
65 precise values of WET for each material in the beam line. Methods for calculating WET
66 in proton beams (IAEA 2000, Newhauser 2001 a, Newhauser *et al* 2007a) and heavy ion
67 beams (IAEA 2000) were proposed previously, but these calculations required either a
68 time-consuming iterative numerical method (NM) or fast but approximate methods of
69 unknown accuracy. We recently derived several analytical formulas for this purpose and

70 showed that these formulas can be used to calculate WET values for materials used in
71 proton therapy of arbitrary density, elemental composition, and thickness with small
72 errors (Zhang and Newhauser 2009).

73 The objectives of this study therefore were to calculate the WET of various
74 materials exposed to beams of protons, helium, carbon and iron ions using the formulas
75 derived in our previous work and to compare our calculations to measured data. The
76 analytical formulas were developed using theoretical range-energy relations, [with the](#)
77 [goal of achieving 1-mm uncertainty in WET.](#)

78

79 **2. Methods and materials**

80 *2.1 Calculation methods*

81 The general formula to calculate WET for heavy charged particle beams is

$$82 \quad \text{WET} = t_w = t_m \frac{\rho_m \bar{S}_m}{\rho_w \bar{S}_w}, \quad (1)$$

83 where t_w and t_m are the thicknesses of water and the target material, respectively; ρ_w and
84 ρ_m are the mass densities of water and the material, respectively; and \bar{S}_w and \bar{S}_m are the
85 mean values of mass stopping power for water and the material, respectively (Newhauser
86 2001). [In essence, WET is the thickness of some medium \$m\$ that causes an ion beam to](#)
87 [lose the same amount of energy as the beam would lose in water.](#) The unitless quantity
88 WER is the ratio of t_w to t_m . The methods for calculating \bar{S} value were extensively
89 described in our previous paper (Zhang and Newhauser 2009) and are explained briefly
90 here for the convenience of the reader.

91 The objective of each of the following three approaches was to calculate the mean
 92 mass stopping power in the material of interest based on relationships between theoretical
 93 mass stopping power and beam energy. The first relationship is based on the Bragg-
 94 Kleeman (BK) rule (Bragg and Kleeman 1905):

$$95 \quad S = -\frac{dE}{\rho dx} \approx -\frac{E^{1-p}}{\rho \alpha p}, \quad (2)$$

96 where α and p are material-dependent constants and E is the initial energy of the heavy
 97 charged particle beam. Values of α and p were obtained by fitting to either residual ranges
 98 or stopping powers data (Ziegler *et al* 1985). A second range-energy relationship for
 99 heavy charged particle beams is captured in the Bethe-Bloch (BB) equation (Bethe 1930,
 100 Bloch 1933):

$$101 \quad S = -\frac{dE}{\rho dx} = 4\pi N_A r_e^2 m_e c^2 z^2 \frac{Z}{A} \frac{1}{\beta^2} \left[\ln \frac{2m_e c^2 \gamma^2 \beta^2}{I} - \beta^2 \right], \quad (3)$$

102 where N_A is Avogadro's number, r_e is the classical electron radius, m_e is the mass
 103 of an electron, z is the charge of projectile, Z is the atomic number of the absorbing
 104 material, A is the atomic weight of the absorbing material, c is speed of light, $\beta = v/c$
 105 where v is the velocity of the projectile, $\gamma = (1 - \beta^2)^{-1/2}$, and I is the mean excitation energy
 106 of the absorbing material, which can be found in the literature (Sternheimer *et al* 1984).
 107 For compounds and mixture materials, the mass fractions of each constituent element are
 108 needed to calculate effective atomic number Z_{eff} , effective atomic weight A_{eff} , and the
 109 effective mean excitation energy, I_{eff} , for the mixture as

$$110 \quad Z_{eff} = \sum a_i Z_i \quad (4)$$

$$111 \quad A_{eff} = \sum a_i A_i \quad (5)$$

112
$$\ln(I_{\text{eff}}) = \frac{\sum_i a_i Z_i \ln(I_i)}{\sum_i a_i Z_i} \quad (6)$$

113 where a_i , Z_i , and I_i are the relative number of moles of element i per mole of compound,
 114 the atomic number, and the mean excitation energy of the i th element in the compound,
 115 respectively (Leo 1987).

116 We previously proposed an empirical formula to calculate I in an empirical form
 117 of the BB equation (EBB) (Zhang and Newhauser 2009), such that $I = kZ$, where $K =$
 118 14.5 when $Z \leq 8$, $K = 13$ when $8 < Z \leq 13$, and $K = 11$ when $Z > 13$.

119 An iterative NM of WET calculation described by Newhauser *et al* (2007a) was
 120 used as one of the standard of comparison for the other analytical formulas used here,
 121 because it is the most exact one of the methods considered.

122 For ‘radiologically thick’ targets (following the definitions of ‘radiologically
 123 thick’ or ‘thin’ from Zhang and Newhauser (2009)), changes in the projectile energy and
 124 mass stopping power must be considered. Therefore, we used \bar{S} instead of point values S
 125 in such cases (the ‘thick-target approach’). \bar{S} values were calculated by integrating
 126 equations (2) and (3) over projectile energy, where the limits of integration were the
 127 projectile energy at the entrance and exit of the slab. \bar{S} value were substituted into
 128 equation (1) to obtain WET values for thick targets. For ‘radiologically thin’ targets, one
 129 may use point value stopping powers established in equation (1) (the ‘thin- target
 130 approach’). However, in this report we included only the thick-target approach for brevity
 131 and because it is the more robust and accurate than the thin-target approach.

132

133 *2.2 Measuring the WET for various materials in heavy charged beams*

134 Proton beam ranges were measured at the Midwest Proton Radiotherapy Institute (MPRI;
135 Bloomington, IN). The MPRI houses a fixed horizontal beam line with a double
136 scattering nozzle and two rotating gantries utilizing uniform scanning nozzles. It was
137 built by the Indiana University Cyclotron Facility which also provides a cyclotron for
138 acceleration of protons to a maximum energy of 208 MeV (Anferov *et al* 2006). All
139 proton experiments described here were performed in the fixed horizontal beam line
140 (Figure 1(a)). The double scattering system includes two scattering foils to spread and
141 flatten the beam. The first foil is made of lead or a combination of lead and polycarbonate,
142 depending upon the beam energy selection. The second foil is made of lead and Lucite.
143 Dose monitoring chambers are used to monitor and adjust the proton beam. Downstream
144 of the scattering foils and the second dose monitoring chamber the beam passes through a
145 range modulator and the snout with a final collimator.

146 A parallel-plate ionization chamber (Markus, model 23343, serial no. 3997, PTW,
147 Freiburg, Germany) coupled with an electrometer (Wellhofer Dosimetrie, model WP5007,
148 serial no. 3245, Nürnberg, Germany) were used to measure the distribution of percentage
149 of dose versus depth using a one-dimensional scanning water phantom system (IBA,
150 model 2001, serial no. 4739, Scanditronix Wellhofer, Bartlett, TN, USA). The beam
151 range was taken as the distal depth along the beam central axis in water corresponding to
152 90% of the maximum dose (D_{\max}) (Gall *et al* 1993). First we measured the range in water
153 without the material of interest in the beam line (R_1); then we measured the range in
154 water with the material placed immediately upstream of the water tank (R_2). WET was
155 the difference of these two ranges (i.e., $R_1 - R_2$). Figure 1 (b) shows the experimental
156 apparatus at the MPRI, including the water tank and a slab of interest.

157 Similar measurements were performed in passively-scattered beams at the
158 Northeast Proton Therapy Center (NPTC, Boston, MA). That system was described in
159 elsewhere (Jongen et al 1996). The WET values for lead were deduced from range
160 measurements made with a parallel-plate ionization chamber (Markus, model 23343,
161 serial no. 2397, PTW, Freiburg, Germany) that was used with a commercial one-
162 dimensional scanning dosimetry system (Computerized Radiation Scanners, model 140,
163 serial no. 311, Vero Beach, FL, USA), which included an electrometer, that was modified
164 for proton therapy applications (Newhauser 2001 a, b). The ionization charge
165 measurements and methods for determination of proton range were described previously
166 (Newhauser *et al* 2002).

167 Table 1 lists the materials used in this study, including gold, lead, stainless steel,
168 titanium, aluminum, polycarbonate resin (Lexan, C₁₆H₁₄O₃, GE Plastics Inc., Pittsfield,
169 MA), polymethylmethacrylate (PMMA) (Lucite, C₅H₈O₂, GE Plastics Inc., Pittsfield,
170 MA), lung substitute plastic (LN300, Gammex RMI, Middleton, WI, USA), polystyrene,
171 high-density polyethylene (HDPE), polyvinylchloride (PVC) and bone substitute plastic
172 (SB3, Gammex RMI, Middleton, WI, USA). Also listed are their mass densities ρ ,
173 $(Z/A)_{\text{eff}}$ values (ratio of Z_{eff} to A_{eff}) and mole fractions. The set of target materials included
174 a wide variety of mass densities and was representative of materials commonly
175 encountered in a charged particle radiotherapy.

176 We tested whether the proton beam field size would affect the beam range results
177 by using different size collimating apertures (with diameters of 10, 8, and 5 cm) with a
178 200-MeV proton beam and with a 10 by 10 cm² aluminum slab present. These
179 measurements were carried out at MPRI.

180 Moyer *et al* (2009) previously measured the WER of different materials used in
181 heavier charged particle beams of various energies at Loma Linda University and the
182 National Aeronautics and Space Administration (NASA) Space Radiation Laboratory at
183 Brookhaven National Laboratory (Upton, NY). These measurements, which were
184 conceptually similar to the range measurements described above, were used in this work
185 to confirm the values predicted using analytical formulas.

186

187 **3. Results**

188 Table 2 lists α and p values for the BK rule for various materials and heavy charged
189 particles. The α values generally decreased with increasing material mass density and
190 atomic number, regardless of the ion type, while the p values were weakly dependent on
191 ion type and target material.

192 The upper portion of table 3 lists the measured WET values that were measured at
193 the MPRI, and the corresponding calculations based on the BK rule and the NM for
194 various materials. The differences between the values predicted by the BK rule and the
195 NM calculations were less than 0.1 mm, and the differences between results predicted by
196 the BK rule and measured data were less than 0.7 mm. Measurements with proton beams
197 of various cross sectional area confirmed that the proton beam range determinations were
198 not influenced by lateral field-size effects. The lower portion of Table 3 lists the
199 measured WET values from the NPTC and the corresponding calculations. Differences
200 between the values of WET from the NM calculations versus those predicted by the BK
201 rule were less than 0.01 mm, and the differences between the values predicted by the BK
202 rule and the values from the measured data were less than 0.3 mm.

203 Table 4, 5 and 6 list WER predictions from the three analytical formulas and the
204 NM for helium, carbon and iron ions in a variety of materials. Compared to the NM as
205 the standard, the BK rule yielded more accurate estimates of WER than the other
206 analytical formulas for most materials and projectile types and energies. For iron ions, the
207 calculated results from three analytical formulas were comparable to one another. The
208 EBB formula yielded WER predictions that were in better agreement with the NM
209 predictions for all ions and absorber materials considered, except for aluminum, where
210 the differences were negligible. This result is consistent with previous comparisons for
211 protons (Zhang and Newhauser 2009). The reason for the superiority of the EBB
212 approach compared to BB is attributable to the empirical approach to estimate I value as
213 presented in section 2.1. The values from tables 4, 5, and 6 also show that helium and
214 heavier projectiles behave in a qualitatively manner similar to that for protons, i.e., the
215 WER values depend on the target material and the beam energy, and the largest
216 deviations from NM occurred when the beam was at the lowest initial energy (Zhang and
217 Newhauser, 2009).

218 It is important to quantify the worst-case errors in WET predictions that were
219 caused by the approximations inherent to the analytical formulas. Figure 2 plots the
220 maximum WET deviations (ΔR_{\max}) for different targets and ion species. More precisely,
221 for a given ion type and target material, ΔR_{\max} is the absolute value of the difference
222 between the WET value from an analytical prediction and the corresponding numerical
223 prediction, or $\Delta R_{\max} = |\text{WET} - \text{WET}_{\text{NM}}|_{\max}$. The range deviations were all less than 1 mm
224 regardless of the target material and ion type, except for the lead target in the helium ion
225 beam, which had range deviations as large as 4.08 mm. In this case, restricting the

226 comparison to 119 MeV/u (MeV per nucleon) and above initial helium ion energy
227 yielded ΔR_{\max} values below 1 mm using the BK rule, while the BB and EBB equations
228 still produced ΔR_{\max} values larger than 1 mm. However, with a slight modification (i.e.,
229 setting $I = 13Z$ for $Z > 13$), the EBB equation also yielded ΔR_{\max} values of less than 0.55
230 mm. Overall, the predictions of WET based on analytical formulas agreed well with the
231 corresponding the NM calculations.

232 Tables 7 lists calculated WER values using the BK rule for proton, carbon ion,
233 and iron ion beams and the corresponding measured values from Moyers *et al* (2009).
234 The data were listed for combinations of different materials, beam types and beam
235 energies. The table also lists the difference between the measured and predicted WET
236 values (WER values were converted to WET values by multiplying the corresponding
237 material thicknesses), denoted by $\Delta R_{\text{BK,exp}}$. Most of the $\Delta R_{\text{BK,exp}}$ values were within 1 mm
238 and all were less than 2.4 mm, and the worst agreement was found for thick targets
239 (thicknesses of 96.5 mm PMMA, 102.9 mm HDPE, 60.07 and 90.14 mm bone substitute
240 slabs, 60.37 mm aluminum).

241

242 **4. Discussion**

243 In this study, WET values of various materials in heavy charged particle beams
244 calculated by one NM and three analytical formulas were validated against measurements.
245 The good agreement between all measured and predicted values (deviations within 1 mm
246 in most cases) provides strong evidence that the analytical methods developed in our
247 previous studies predicts WET values with adequate accuracy for various [clinically-](#)
248 [relevant](#) ion species, ion energies, and absorber materials.

249 The International Atomic Energy Agency (IAEA) has proposed techniques to
250 predict the approximate WET of plastic phantoms used for relative proton dosimetry
251 using the ratio of the continuous-slowing-down approximation (CSDA) range (in g cm^{-2})
252 in water to that in the material of interest; and to predict the approximate WET of plastic
253 phantoms used in heavy-ion beam dosimetry (atomic numbers between 2 and 18) as the
254 product of the phantom thickness and the mass density of the phantom (IAEA 2000).
255 Because the CSDA range represents complete loss of ion energy, meaning that the target
256 thickness must be larger than the beam range, this approximation is not applicable in
257 many clinical situations where WET values are needed. Our finding suggests that the
258 simple analytical WET formulas from Zhang and Newhauser (2009), which were
259 developed for protons passing through absorbers of arbitrary thickness and composition,
260 also provide more accurate predictions for helium, carbon and iron ions than those that
261 can be achieved using the IAEA method. The main differences are: the analytical
262 formulas can be used for thick targets; the calculation uncertainties and the interval of
263 applicable energies are now known.

264 The results of this study have several applications. The analytical formulas used
265 here may be useful in configuring treatment planning systems rather than complex
266 numerical methods; the thicknesses of several radiologically thick components in the
267 treatment head are specified in the planning system in terms of WET (Newhauser *et al*
268 2007c, Kramer *et al* 2000). The analytical formulas may also be particularly useful in
269 calculating WET values for metal implants in patients (Newhauser *et al* 2007a, b, 2008).
270 Our results can also be used in heavy charged particle beam dosimetry because the
271 absorbed dose measurements depend on the geometric relationships between the particle

272 beam and equipment in the treatment head, and their geometric dimensions are often
273 specified as WET (Newhauser *et al* 2001 a, b, Newhauser *et al* 2002, IAEA 2000).
274 While our methods are adequate for many clinical calculations, the requirements on the
275 accuracy of WET predictions depend on many factors, including the treatment site,
276 treatment technique, and the proximity of nearby critical structures.

277 This study had several limitations. First, we neglected density and shell
278 corrections in the BB equation for heavy charged particles following the methods of the
279 previous study on proton WET calculations (Zhang and Newhauser 2009). The calculated
280 results in this paper show this approximation still yields good accuracy in clinical
281 environments and therefore it is not a serious limitation. Second, the EBB equation
282 required modification of the empirical equation used to calculate I so that errors were less
283 than 1 mm for the case of the lead target in the helium ion beam. Because this was a rare
284 occurrence, the analytical formula is still applicable in most cases. Third, we did not
285 verify the thin-target approach for heavy charged particle beams other than proton beams
286 (The thin-target approach were tested for proton beam in our previous study (Zhang and
287 Newhauser 2009)).

288 In conclusion, we have confirmed that analytical formulas of thick-target
289 approach can be used to calculate WET values of various types of materials in beams of
290 protons, helium, carbon and iron ions with high accuracy. This finding is important
291 because of the increasing use of heavy charged particle beams for cancer treatment and
292 the need for accurate predictions of WET values for such therapies.

293

294 **Acknowledgments**

295 We thank Brian Allen and Draik Hecksel at the MPRI for their assistance with the proton
296 WET measurements, Dr. Michael Moyers for the helpful discussions, Dr. Uwe Titt for
297 providing lung tissue equivalent material, and Kathryn B. Carnes for her assistance in
298 preparing this manuscript. This work was supported in part by Northern Illinois
299 University through a subcontract of a Department of Defense contract (award W81XWH-
300 08-1-0205) and by the National Cancer Institute (award 1 R01 CA131463-01A1).

301

302 **References**

303 Amaldi U and Kraft G 2005 Radiotherapy with beams of carbon ions *Rep. Prog. Phys.* **68**
304 1861-82

305 Anferov V, Collins J, Friesel D L, Katuin J, Klein S B, Nichiporov D and Wedekind M
306 W 2006 The Indiana University proton therapy system *Proceedings of EPAC*.
307 (Edinburgh, Scotland) WEPOCH179, 2349-51 <http://accelconf.web.cern.ch/AccelConf/e06/>

308 Bethe H 1930 Zur Theorie des Durchgangs schneller Korpuskularstrahlen durch Materie
309 *Ann. Physik.* **5** 324-400

310 Bloch F 1933 Zur Bremsung rasch bewegter Teilchen beim Durchgang durch Materie
311 *Ann. Physik.* **16** 285-320

312 Bragg W and Kleemann R 1905 On the alpha heavy charged particles of radium and their
313 loss of range in passing through various atoms and molecules *Phil. Mag.* **10** 318-40

314 Gall K P, Verhey L, Alonso J, Castro J, Collier J M, Chu W, Daftari I, Goitein M, Kubo
315 H, Ludewigt B, Munzenrider J, Petti P, Renner T, Rosenthal S, Smith A, Staples J,
316 Suit H and Thornton A 1993 State of the art? New proton medical facilities for the

317 Massachusetts General Hospital and the University of California Davis medical
318 Center *Nucl. Instrum. Methods. Phys. Res.* **B79** 881-4

319 Goitein M, Lomax A and Pedroni E 2002 Treating cancer with protons *Phys. Today.* **55**
320 45-50

321 IAEA 2000 Absorbed dose determination in external beam radiotherapy *IAEA Technical*
322 *Report Series* 398 (Vienna: International Atomic Energy Agency)

323 Jakel O, Schulz-Ertner D, Karger C P, Nikoghosyan A and Debus J 2003 Heavy ion
324 therapy: status and perspectives *Technology in Cancer Research and Treatment.* **2**
325 377-87

326 Jongen Y, Beeckman W and Cohilis P 1996 The proton therapy system for MGH's NPTC:
327 equipment description and progress report *Bull. Cancer. Radiother.* **83** 219s-22s.

328 Kramer M, Jakel O, Haberer T, Kraft G, Schardt D and Weber U 2000 Treatment
329 planning for heavy-ion radiotherapy: physical beam model and dose optimization
330 *Phys. Med. Biol.* **45** 3299-317

331 Leo W R 1987 *Techniques for Nuclear and Particle Physics Experiments* (Berlin:
332 Springer)

333 Moyers F M 2009 Ion stopping powers and CT numbers *Medical Dosimetry* in press

334 Newhauser W 2001a Dosimetry for the gantry beams at the northeast proton therapy
335 center: Part I. Dimensions and geometric relationships *Massachusetts General*
336 *Hospital Report HD-112*

337 Newhauser W 2001b Proton field calibration measurements and analysis with the
338 calibrationsetup program (CSU) Version 1.1 *Massachusetts General Hospital*
339 *Report*

340 Newhauser W, Myers K D, Rosenthal S J and Smith A R 2002 Proton beam dosimetry
341 for radiosurgery: implementation of the ICRU Report 59 at the Harvard Cyclotron
342 Laboratory *Phys. Med. Biol.* **47** 1369-89

343 Newhauser W, Fontenot J, Koch N, Dong L, Lee A, Zheng Y, Waters L and Mohan R
344 2007a Monte Carlo simulations of the dosimetric impact of radiopaque fiducial
345 markers for proton radiotherapy of the prostate *Phys. Med. Biol.* **52** 2937-52

346 Newhauser W D, Koch N C, Fontenot J D, Rosenthal S J, Gombos D S, Fitzek M M and
347 Mohan R 2007b Dosimetric impact of tantalum markers used in the treatment of
348 uveal melanoma with proton beam therapy *Phys. Med. Biol.* **52** 3979-90

349 Newhauser W, Fontenot J, Zheng Y, Polf J, Titt U, Koch N, Zhang X and Mohan R
350 2007c Monte carlo simulations for configuring and testing an analytical proton
351 dose-calculation algorithm *Phys. Med. Biol.* **52** 4569-84

352 Newhauser W D, Giebeler A, Langen K M, Mirkovic D and Mohan R. 2008 Can
353 megavoltage computed tomography reduce proton range uncertainties in treatment
354 plans for patients with large metal implants? *Phys. Med. Biol.* **53** 2327-44

355 Schulz-Ertner D, Jakel O and Schlegel W 2006 Radiation therapy with charged particles
356 *Semin. Radiat. Oncol.* **16** 249-59

357 Schulz-Ertner D and Tsujii H 2007 Particle radiation therapy using proton and heavier
358 ion beams *J. Clin. Oncol.* **25** 953-64

359 Sternheimer R M, Berger M J and Seltzer S M 1984 Density effect for the ionization loss
360 of charged particles in various substances *At. Data Nucl. Data Tables* **30** 261-71

361 Wilson R R 1946 Radiological use of fast protons *Radiology* **47** 487-91

362 Yepes P, Randeniya S, Taddei P and Newhauser W 2009 Monte Carlo fast dose
363 calculator for proton radiotherapy: application to a voxelized geometry
364 representing a patient with prostate cancer. *Phys. Med. Biol.* **54** N21-28.

365 Zhang R and Newhauser W D 2009 Calculation of water equivalence of materials of
366 arbitrary density, elemental composition and thickness in proton beam irradiation
367 *Phys. Med. Biol.* **54** 1383-95

368 Ziegler J F, Biersack J P and Littmark U 1985 *The Stopping and Ranges of Ions in Solids*
369 (New York: Pergamon)

370

371

372

373

374

375

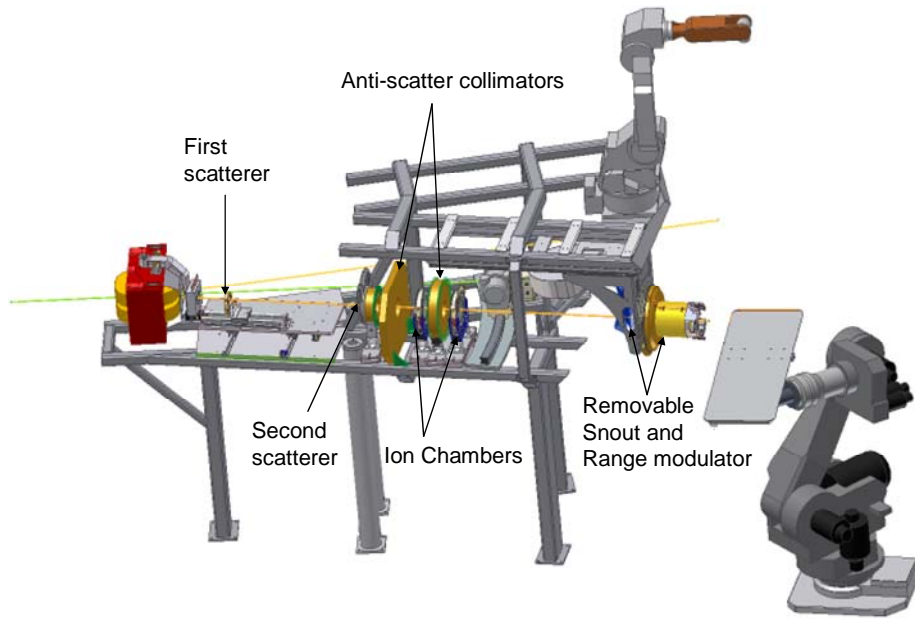
376

377

378

379

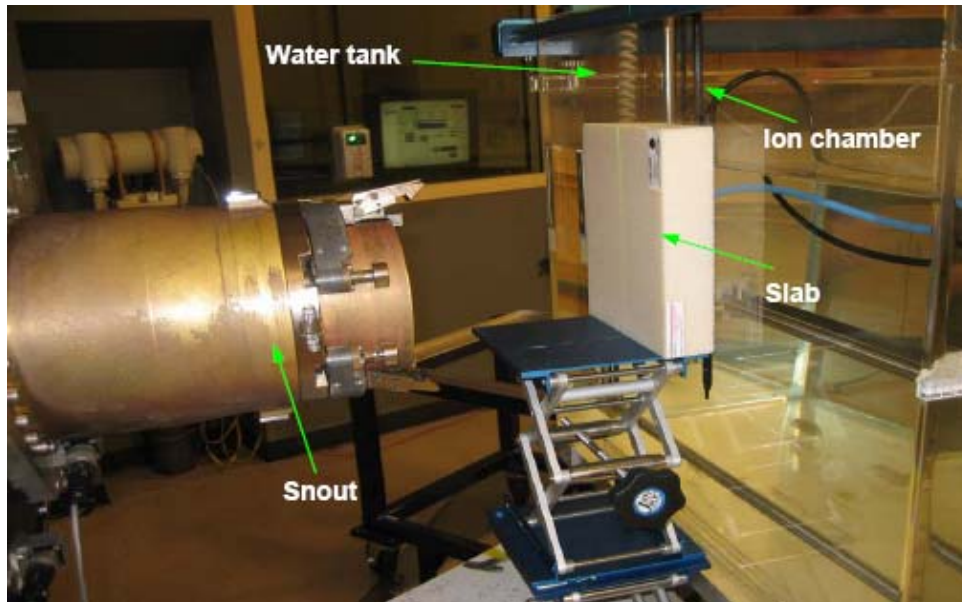
380



381

382

(a)



383

384

(b)

385 **Figure 1.** (a) Schematic diagram of the fixed horizontal proton beam line configuration at
 386 the MPRI (Courtesy of Indiana University Cyclotron Facility). (b) Experimental
 387 apparatus at the end of the proton beam line at the MPRI for measuring the WET of one
 388 material (a lung substitute plastic slab).

389

390 **Table 1.** Common materials used in heavy charged particle beams, with their mass
 391 densities ρ , values of $(Z/A)_{\text{eff}}$, and mole fractions.

Material	ρ (g/cm ³)	$(Z/A)_{\text{eff}}$	Mole fraction (%)
Lung substitute	0.3	0.537	H 55.577, C 32.738, N 0.927, O 7.508, Cl 0.019, Si 0.184, Mg 3.048
HDPE	0.964	0.570	H 66.717, C 33.283
Water	1.0	0.555	H 66.667, O 33.333
Polystyrene	1.06	0.538	H 49.851, C 50.149
PMMA	1.185	0.539	H 53.333, C 33.333, O 13.333,
Lexan	1.20	0.527	H 42.424, C 48.485, O 9.091
PVC	1.385	0.512	H 50.218, C 33.202, Cl 16.580
Bone substitute	1.829	0.516	H 35.215, C 29.592, N 0.803, O 26.695, Cl 0.16, Ca 7.679
Aluminum	2.698	0.482	Al 100
Titanium	4.519	0.459	Ti 100
Stainless steel	7.85	0.466	C 0.045, N 0.045, Si 0.450, Cr 18.150, Mn 1.250, Fe 71.460, Ni 8.550, Mo 0.050
Lead	11.322	0.396	Pb 100
Gold	19.311	0.401	Au 100

392

393

394

395

396

397

398

399 **Table 2.** Fitting parameters of α and p for various materials when applying the BK rule.
 400 The energies used in the fit were from 10 to 250 MeV for proton beams, 25 to 1000 MeV
 401 for helium ions, 250 to 10000 MeV for carbon ions and iron ions.

Material	Proton		Helium		Carbon		Iron	
	α	p	α	p	α	p	α	p
Lung	$8.994 \cdot 10^{-3}$	1.735	$7.420 \cdot 10^{-4}$	1.748	$1.908 \cdot 10^{-4}$	1.545	$8.421 \cdot 10^{-7}$	1.715
HDPE	$2.541 \cdot 10^{-3}$	1.737	$2.380 \cdot 10^{-4}$	1.738	$5.352 \cdot 10^{-5}$	1.548	$2.337 \cdot 10^{-7}$	1.719
Water	$2.633 \cdot 10^{-3}$	1.735	$2.367 \cdot 10^{-4}$	1.735	$5.605 \cdot 10^{-5}$	1.545	$2.443 \cdot 10^{-7}$	1.716
Polystyrene	$2.545 \cdot 10^{-3}$	1.735	$2.285 \cdot 10^{-4}$	1.736	$5.378 \cdot 10^{-5}$	1.546	$2.314 \cdot 10^{-7}$	1.719
PMMA	$2.271 \cdot 10^{-3}$	1.735	$2.039 \cdot 10^{-4}$	1.736	$4.814 \cdot 10^{-5}$	1.545	$2.161 \cdot 10^{-7}$	1.714
Lexan	$2.310 \cdot 10^{-3}$	1.735	$2.067 \cdot 10^{-4}$	1.736	$4.838 \cdot 10^{-5}$	1.546	$2.145 \cdot 10^{-7}$	1.716
Bone substitute	$1.666 \cdot 10^{-3}$	1.730	$1.502 \cdot 10^{-4}$	1.731	$3.566 \cdot 10^{-5}$	1.540	$1.543 \cdot 10^{-7}$	1.714
Aluminum	$1.364 \cdot 10^{-3}$	1.719	$1.257 \cdot 10^{-4}$	1.719	$2.897 \cdot 10^{-5}$	1.534	$1.432 \cdot 10^{-7}$	1.694
Titanium	$9.430 \cdot 10^{-4}$	1.710	$8.721 \cdot 10^{-5}$	1.712	$1.949 \cdot 10^{-5}$	1.531	$1.084 \cdot 10^{-7}$	1.679
Stainless steel	$5.659 \cdot 10^{-4}$	1.706	$5.159 \cdot 10^{-5}$	1.707	$1.173 \cdot 10^{-5}$	1.525	$6.273 \cdot 10^{-8}$	1.678
Lead	$6.505 \cdot 10^{-4}$	1.676	$6.357 \cdot 10^{-5}$	1.676	$1.438 \cdot 10^{-5}$	1.499	$7.887 \cdot 10^{-8}$	1.656
Gold	$3.705 \cdot 10^{-4}$	1.677	$3.628 \cdot 10^{-5}$	1.677	$8.053 \cdot 10^{-6}$	1.502	$5.495 \cdot 10^{-8}$	1.633

402
 403
 404
 405
 406
 407
 408
 409
 410
 411
 412

413 **Table 3.** WET values from the numerical method (WET_{NM}), the BK rule (WET_{BK}) and
414 experiments (WET_{exp}) for various materials with different thickness (t_m) and proton beam
415 energies (E_i). The difference between the results predicted by the BK rule and the
416 numerical method ($\Delta R_{BK, NM}$), and the difference between the results predicted by the BK
417 rule the measured data ($\Delta R_{BK, exp}$) were also listed.

418

Material	E_i (MeV)	t_m (mm)	WET_{NM} (mm)	WET_{BK} (mm)	WET_{exp} (mm)	$\Delta R_{BK, NM}$ (mm)	$\Delta R_{BK, exp}$ (mm)
Lead	200	18.72	106.0	106.0	106.1	0.1	-0.1
	200	13.27	75.3	75.4	75.9	0.1	0.5
	200	5.45	31.0	31.1	30.8	0.1	0.3
Aluminum	100	5.45	29.8	29.7	29.3	-0.1	0.4
	200	19.73	41.6	41.7	42.3	0.1	-0.6
	200	14.90	31.4	31.5	32.2	0.1	-0.7
	200	4.83	10.2	10.2	10.4	0.0	-0.2
PMMA	100	14.90	31.1	31.1	31.5	0.0	-0.4
	100	4.83	10.1	10.1	10.3	0.0	-0.2
	200	110.13	127.5	127.5	127.7	0.0	-0.2
	200	99.96	115.7	115.7	115.9	0.0	-0.2
Polystyrene	200	10.17	11.8	11.8	11.8	0.0	0.0
	100	10.17	11.8	11.8	12.0	0.0	-0.2
	200	49.83	51.3	51.3	50.9	0.0	0.4
Lung substitute	100	49.83	51.3	51.3	51.1	0.0	0.2
	200	40.09	11.7	11.7	11.8	0.0	-0.1
Lead	100	40.09	11.7	11.7	11.8	0.0	-0.1
	172.2	0.03	0.17	0.17	0.32	0.0	-0.15
Lexan	172.2	0.06	0.34	0.34	0.31	0.0	0.03
	172.2	0.125	0.71	0.71	0.74	0.0	0.03
	172.2	0.25	1.42	1.42	1.13	0.0	0.29
	172.2	0.5	2.84	2.83	2.88	-0.01	-0.05
	172.2	1.0	5.67	5.66	5.64	-0.01	0.02
	172.2	5.48	6.25	6.25	6.14	0.0	0.11
	172.2	2.74	3.12	3.12	3.12	0.0	0.0
	172.2	1.37	1.56	1.56	1.56	0.0	0.0

419

420

421

422

423

424

425 **Table 4.** For helium ions, the values of WER calculated using the analytical formulas
 426 (BK, BB, and EBB) and NM for various materials as a function of the material thickness,
 427 beam energy (E_i , MeV per nucleon, MeV/u), and the corresponding residual range in
 428 water (R_w). Dashes indicate that the helium beam stopped in the target.

E_i (MeV/u)	R_w (cm)	WER											
		1.5 cm lead				2 cm aluminum				10 cm PMMA			
		NM	BK	BB	EBB	NM	BK	BB	EBB	NM	BK	BB	EBB
75	4.59	-	-	-	-	2.068	2.062	2.101	2.101	-	-	-	-
81.25	5.3	-	-	-	-	2.077	2.071	2.108	2.108	-	-	-	-
87.5	6.06	-	-	-	-	2.082	2.076	2.112	2.112	-	-	-	-
93.75	6.85	-	-	-	-	2.086	2.080	2.115	2.115	-	-	-	-
100	7.69	-	-	-	-	2.089	2.084	2.118	2.118	-	-	-	-
106.25	8.57	5.377	5.278	5.613	5.533	2.092	2.087	2.120	2.120	-	-	-	-
112.5	9.49	5.426	5.358	5.688	5.610	2.094	2.089	2.122	2.122	-	-	-	-
118.75	10.44	5.457	5.407	5.729	5.653	2.096	2.092	2.124	2.124	-	-	-	-
125	11.43	5.487	5.445	5.758	5.683	2.098	2.094	2.125	2.125	-	-	-	-
131.25	12.46	5.511	5.476	5.782	5.708	2.099	2.096	2.126	2.126	1.159	1.158	1.167	1.159
137.5	13.52	5.532	5.503	5.801	5.728	2.101	2.098	2.128	2.128	1.158	1.158	1.167	1.158
143.75	14.62	5.551	5.526	5.818	5.745	2.102	2.100	2.129	2.129	1.158	1.158	1.166	1.158
150	15.75	5.568	5.548	5.833	5.761	2.103	2.101	2.130	2.130	1.158	1.158	1.166	1.158
156.25	16.91	5.584	5.568	5.847	5.775	2.105	2.103	2.131	2.131	1.158	1.158	1.166	1.158
162.5	18.11	5.599	5.586	5.859	5.787	2.106	2.104	2.132	2.132	1.158	1.158	1.166	1.158
168.75	19.33	5.614	5.603	5.870	5.799	2.107	2.106	2.133	2.133	1.158	1.158	1.166	1.158
175	20.58	5.626	5.620	5.881	5.810	2.108	2.107	2.133	2.134	1.158	1.158	1.166	1.158
181.25	21.87	5.639	5.635	5.891	5.820	2.109	2.109	2.134	2.134	1.158	1.158	1.166	1.158
187.5	23.19	5.651	5.649	5.900	5.830	2.110	2.110	2.135	2.135	1.158	1.158	1.166	1.158
193.75	24.53	5.663	5.663	5.909	5.839	2.111	2.111	2.136	2.136	1.158	1.157	1.166	1.158
200	25.91	5.674	5.676	5.917	5.847	2.111	2.112	2.136	2.137	1.158	1.157	1.166	1.158
206.25	27.31	5.684	5.689	5.925	5.856	2.112	2.113	2.137	2.137	1.157	1.157	1.165	1.158
212.5	28.74	5.694	5.701	5.932	5.863	2.113	2.115	2.138	2.138	1.157	1.157	1.165	1.158
218.75	30.2	5.704	5.712	5.940	5.871	2.114	2.116	2.138	2.139	1.157	1.157	1.165	1.158
225	31.69	5.714	5.724	5.946	5.878	2.114	2.117	2.139	2.139	1.157	1.157	1.165	1.158
231.25	33.19	5.723	5.734	5.953	5.885	2.115	2.118	2.140	2.140	1.157	1.157	1.165	1.158
237.5	34.72	5.732	5.745	5.960	5.891	2.116	2.119	2.140	2.140	1.157	1.157	1.165	1.158
243.75	36.27	5.740	5.755	5.966	5.898	2.116	2.119	2.141	2.141	1.157	1.157	1.165	1.158
250	37.85	5.749	5.765	5.972	5.904	2.117	2.120	2.141	2.141	1.157	1.157	1.165	1.158

429

430

431

432

433

434 **Table 5.** For carbon ions, the values of WER calculated using the analytical formulas
 435 (BK, BB, and EBB) and NM for various materials as a function of the material thickness,
 436 beam energy (E_i , MeV per nucleon, MeV/u), and the corresponding residual range in
 437 water (R_w). Dashes indicate that the carbon beam stopped in the target.

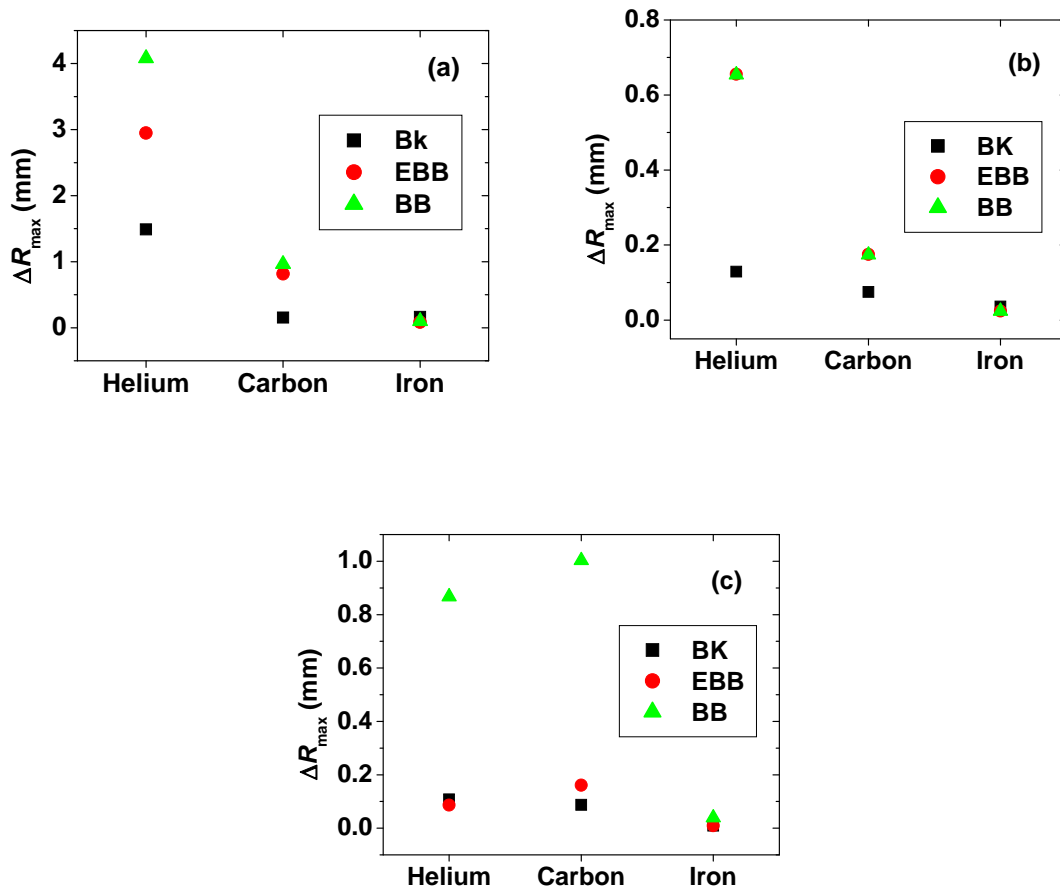
E_i (MeV/u)	R_w (cm)	WER											
		1.2 cm lead				1.5 cm aluminum				10 cm PMMA			
		NM	BK	BB	EBB	NM	BK	BB	EBB	NM	BK	BB	EBB
125	3.81	-	-	-	-	2.09	2.095	2.102	2.102	-	-	-	-
145.83	4.99	-	-	-	-	2.099	2.101	2.109	2.109	-	-	-	-
166.67	6.3	-	-	-	-	2.104	2.105	2.114	2.114	-	-	-	-
187.5	7.72	5.57	5.583	5.647	5.568	2.108	2.109	2.118	2.118	-	-	-	-
208.33	9.26	5.631	5.641	5.711	5.635	2.111	2.112	2.121	2.121	-	-	-	-
229.17	10.88	5.675	5.684	5.754	5.679	2.114	2.114	2.124	2.124	-	-	-	-
250	12.61	5.712	5.720	5.787	5.713	2.116	2.116	2.126	2.126	1.157	1.158	1.167	1.159
270.83	14.41	5.743	5.749	5.814	5.741	2.118	2.118	2.128	2.128	1.158	1.158	1.167	1.158
291.67	16.29	5.771	5.776	5.836	5.764	2.12	2.120	2.130	2.130	1.157	1.158	1.166	1.158
312.5	18.27	5.796	5.799	5.856	5.785	2.122	2.122	2.131	2.131	1.157	1.157	1.166	1.158
333.33	20.33	5.819	5.821	5.874	5.803	2.123	2.123	2.133	2.133	1.157	1.157	1.166	1.158
354.17	22.42	5.841	5.840	5.890	5.819	2.125	2.125	2.134	2.134	1.157	1.157	1.166	1.158
375	24.58	5.86	5.859	5.905	5.835	2.126	2.126	2.135	2.135	1.157	1.157	1.166	1.158
395.83	26.82	5.878	5.876	5.918	5.848	2.127	2.128	2.136	2.137	1.157	1.157	1.166	1.158
416.67	29.13	5.895	5.892	5.930	5.861	2.129	2.129	2.138	2.138	1.157	1.157	1.165	1.158
437.5	31.46	5.911	5.907	5.942	5.873	2.13	2.130	2.139	2.139	1.157	1.157	1.165	1.158
458.33	33.85	5.926	5.921	5.953	5.885	2.131	2.131	2.140	2.140	1.157	1.157	1.165	1.158
479.17	36.31	5.94	5.934	5.963	5.896	2.132	2.132	2.140	2.141	1.157	1.157	1.165	1.158
500	38.83	5.953	5.947	5.973	5.906	2.133	2.133	2.141	2.142	1.157	1.157	1.165	1.158
520.83	41.35	5.965	5.959	5.983	5.915	2.134	2.134	2.142	2.142	1.157	1.157	1.165	1.158
541.67	43.93	5.977	5.971	5.992	5.925	2.135	2.135	2.143	2.143	1.157	1.157	1.165	1.158
562.5	46.56	5.988	5.982	6.000	5.933	2.136	2.136	2.144	2.144	1.157	1.157	1.165	1.158
583.33	49.24	5.999	5.993	6.008	5.942	2.136	2.137	2.145	2.145	1.157	1.157	1.165	1.158
604.17	51.92	6.009	6.003	6.016	5.950	2.137	2.137	2.145	2.145	1.157	1.157	1.165	1.158
625	54.65	6.018	6.013	6.024	5.958	2.138	2.138	2.146	2.146	1.157	1.157	1.165	1.158
645.83	57.43	6.027	6.023	6.031	5.965	2.139	2.139	2.147	2.147	1.157	1.157	1.165	1.157
666.67	60.25	6.036	6.032	6.038	5.973	2.139	2.140	2.147	2.147	1.157	1.157	1.165	1.157
687.5	63.05	6.044	6.041	6.045	5.980	2.14	2.140	2.148	2.148	1.157	1.157	1.165	1.157
708.33	65.89	6.052	6.050	6.051	5.987	2.141	2.141	2.149	2.149	1.157	1.157	1.165	1.157
729.17	68.78	6.059	6.058	6.058	5.993	2.141	2.142	2.149	2.149	1.156	1.157	1.165	1.157
750	71.7	6.066	6.066	6.064	6.000	2.142	2.142	2.150	2.150	1.156	1.157	1.164	1.157
770.83	74.61	6.073	6.074	6.070	6.006	2.143	2.143	2.150	2.150	1.156	1.157	1.164	1.157
791.67	77.56	6.08	6.082	6.076	6.012	2.143	2.144	2.151	2.151	1.156	1.157	1.164	1.157
812.5	80.54	6.086	6.090	6.082	6.018	2.144	2.144	2.151	2.152	1.156	1.156	1.164	1.157
833.33	83.55	6.092	6.097	6.088	6.024	2.144	2.145	2.152	2.152	1.156	1.156	1.164	1.157

438

439 **Table 6.** For iron ions, the values of WER calculated using the analytical formulas (BK,
440 BB, and EBB) and NM for various materials as a function of the material thickness, beam
441 energy (E_i , MeV per nucleon, MeV/u), and the corresponding residual range in water (R_w).
442 Dashes indicate that the iron beam stopped in the target.

E_i (MeV/u)	R_w (cm)	WER											
		0.1 cm lead				0.2 cm aluminum				0.3 cm PMMA			
		NM	BK	BB	EBB	NM	BK	BB	EBB	NM	BK	BB	EBB
71.43	0.37	-	-	-	-	-	-	-	-	1.157	1.155	1.170	1.160
75	0.4	-	-	-	-	-	-	-	-	1.159	1.156	1.169	1.160
78.57	0.44	-	-	-	-	2.064	2.046	2.072	2.072	1.158	1.156	1.169	1.160
82.14	0.47	-	-	-	-	2.071	2.056	2.082	2.082	1.158	1.156	1.169	1.159
85.71	0.51	-	-	-	-	2.076	2.063	2.087	2.087	1.158	1.157	1.168	1.159
89.29	0.54	5.273	5.110	5.280	5.188	2.08	2.068	2.091	2.091	1.158	1.157	1.168	1.159
92.86	0.58	5.329	5.185	5.382	5.293	2.082	2.072	2.093	2.094	1.158	1.157	1.168	1.159
96.43	0.62	5.368	5.230	5.436	5.349	2.084	2.075	2.096	2.096	1.158	1.157	1.168	1.159
100	0.66	5.393	5.264	5.473	5.388	2.087	2.078	2.098	2.098	1.158	1.157	1.168	1.159
103.57	0.7	5.416	5.292	5.503	5.419	2.088	2.081	2.100	2.100	1.158	1.158	1.168	1.159
107.14	0.74	5.438	5.316	5.527	5.444	2.09	2.084	2.101	2.101	1.158	1.158	1.168	1.159
110.71	0.79	5.453	5.337	5.547	5.465	2.092	2.086	2.103	2.103	1.158	1.158	1.168	1.159
114.29	0.83	5.471	5.356	5.566	5.484	2.093	2.088	2.104	2.104	1.158	1.158	1.168	1.159
117.86	0.88	5.484	5.374	5.582	5.501	2.095	2.090	2.105	2.105	1.158	1.158	1.167	1.159
121.43	0.92	5.497	5.390	5.596	5.516	2.096	2.092	2.106	2.107	1.158	1.158	1.167	1.159
125	0.97	5.51	5.405	5.610	5.529	2.097	2.094	2.108	2.108	1.158	1.158	1.167	1.159
128.57	1.02	5.522	5.419	5.622	5.542	2.098	2.096	2.109	2.109	1.158	1.158	1.167	1.159
132.14	1.07	5.532	5.433	5.633	5.554	2.099	2.098	2.110	2.110	1.158	1.159	1.167	1.159
135.71	1.12	5.544	5.445	5.644	5.565	2.1	2.099	2.110	2.111	1.158	1.159	1.167	1.159
139.29	1.17	5.554	5.457	5.654	5.575	2.101	2.101	2.111	2.111	1.158	1.159	1.167	1.159
142.86	1.22	5.563	5.469	5.664	5.585	2.101	2.102	2.112	2.112	1.158	1.159	1.167	1.159
146.43	1.28	5.572	5.480	5.672	5.594	2.102	2.104	2.113	2.113	1.158	1.159	1.167	1.159
150	1.33	5.581	5.491	5.681	5.603	2.103	2.105	2.114	2.114	1.158	1.159	1.167	1.159
153.57	1.38	5.59	5.501	5.689	5.612	2.104	2.106	2.114	2.114	1.158	1.159	1.167	1.159
157.14	1.44	5.598	5.511	5.697	5.620	2.104	2.108	2.115	2.115	1.158	1.159	1.167	1.159
160.71	1.5	5.607	5.521	5.704	5.627	2.105	2.109	2.116	2.116	1.158	1.159	1.167	1.158
164.29	1.55	5.614	5.530	5.711	5.635	2.106	2.110	2.116	2.116	1.158	1.159	1.167	1.158
167.86	1.61	5.621	5.539	5.718	5.642	2.107	2.111	2.117	2.117	1.158	1.159	1.167	1.158
171.43	1.67	5.629	5.548	5.724	5.648	2.107	2.112	2.117	2.118	1.158	1.159	1.167	1.158
175	1.73	5.636	5.556	5.731	5.655	2.108	2.113	2.118	2.118	1.158	1.160	1.167	1.158
178.57	1.79	5.643	5.564	5.737	5.661	2.108	2.115	2.119	2.119	1.158	1.160	1.167	1.158

443



444

445

446 **Figure 2.** Maximum deviations, ΔR_{\max} , in WET values calculated by the analytical
 447 formulas relative to that given by the NM for (a) lead, (b) aluminum, and (c) PMMA. The
 448 thicknesses of materials used were: 1.5 cm lead, 2 cm aluminum, and 10 cm PMMA for
 449 helium ions; 1.2 cm lead, 1.5 cm aluminum, and 10 cm PMMA for carbon ions; 0.1 cm
 450 lead, 0.2 cm aluminum, and 0.3 cm PMMA for iron ions.

451

452

453

454

455 **Table 7.** Calculated (using the BK rule) and measured (Moyers *et al* 2009) WER values
 456 of various materials with different thickness (t_m).in proton beams, carbon ions and iron
 457 ions at certain energies (E_i), and the difference between the results predicted by the BK
 458 rule and the measured data ($\Delta R_{BK, exp}$).

459

Particle	Material	t_m (mm)	E_i (MeV/u)	WER		$\Delta R_{BK, exp}$ (mm)
				BK	Measurement	
Proton	Aluminum	19.3	135	2.097	2.130 ± 1.49	-0.637
			175	2.107	2.114 ± 1.49	-0.135
			225	2.116	2.145 ± 1.49	-0.560
	PMMA	96.5	135	1.158	1.170 ± 0.46	-1.158
			175	1.158	1.162 ± 0.46	-0.386
			225	1.158	1.167 ± 0.46	-0.869
	HDPE	102.9	135	1.023	1.036 ± 0.47	-1.338
			175	1.022	1.031 ± 0.47	-0.926
			225	1.021	1.035 ± 0.47	-1.441
	PVC	37	135	1.224	1.232 ± 1.14	-0.296
			175	1.227	1.232 ± 1.14	-0.185
			225	1.229	1.254 ± 1.14	-0.925
	Bone substitute	30.1	135	1.625	1.635 ± 1.15	-0.301
			175	1.627	1.615 ± 1.15	0.361
			225	1.630	1.631 ± 1.15	-0.030
Carbon	Aluminum	40.28	290	2.117	2.125 ± 0.72	-0.322
	HDPE	100.27	290	1.020	1.021 ± 0.49	-0.100
	Bone substitute	60.07	290	1.630	1.613 ± 0.58	1.021
Iron	Aluminum	60.37	970	2.192	2.153 ± 0.47	2.354
	PMMA	95.23	970	1.165	1.165 ± 0.47	0.0
	HDPE	150.44	970	1.017	1.017 ± 0.33	0.0
	Bone substitute	90.14	970	1.632	1.620 ± 0.38	1.082

460

461